COMPARATIVE ANALYSIS OF A STRUCTURAL REPAIR IN A LIGHT AIRCRAFT'S FUSELAGE USING FINITE ELEMENT METHOD

André Santiago Beires[1]

Thiago Augusto Machado Guimarães[1]

Giuliano Gardolinski Venson[1]

Adriano Correa do Couto[2]

asbeires@gmail.com

thiago@femec.ufu.br

venson@femec.ufu.br

adriano.couto@algaraviation.com.br

[1] Federal University of Uberlândia, School of Mechanical Engineering, Laboratory of Mechanics and Structures (LMEst). Av. João Naves de Ávila 2121, Uberlândia, MG. Brasil.

[2] Algar Aviation Taxi Aéreo S/A. Aeroporto de Uberlândia. Hangar Walter Garcia. Uberlândia, MG, Brasil.

Abstract. *The purpose of this paper is to analyze the structural repair that was designed for an aircraft, which accidentally landed without landing gears and damaged the fuselage lower skin near wing junction. As the manufacturer of the aircraft in discussion doesn't provide a structural repair solution to evaluate the repair design, a comparative finite element analysis (FEA) was done in order to check airworthiness conditions, load path and stress distribution between the original structure (without repair) and the modified structure (with repair). The whole analysis process involves: geometry construction of all components in the affected area including the attachment parts, finite element model creation, structural analysis comparison and the compliance demonstration with FAR 23 structural requirements.*

Keywords: *Structural repair, finite element analysis, airworthiness condition, stress distribution, load path.*

1 INTRODUCTION

During the aircraft designing phase the optimal result is a compromise solution between technical and economic constraints (L. Reimer et. al, 2009). It is a common industry practice to design structural parts through finite element analysis. Z.Q. Guan (2003) states that this kind of analysis has important guiding significance and practical value that can improve product quality and performance, reduce production costs, shorten design cycle and so on. To examine the use of such methods in the aeronautical industry, a static analysis of a structural repair designed for a damaged aircraft is described.

The repaired aircraft used in the study is a TBM 700 that belongs to a private owner, which is a high performance single-engine turboprop light business and utility aircraft (Figure 1). Manufactured by the French company DAHER-SOCATA with pressurized cabin, the TBM 700 is optimized to compete with twin-engine aircrafts of similar sizes.

Figure 1. Aircraft SOCATA TBM 700

The aircraft was damaged after an unsuccessful landing, where the landing gear was not extended providing contact between the fuselage lower skin and the ground. Details of the damaged aircraft can be seen in Figure 2. The accident caused damages to some components, mainly in the external skin and longitudinal stiffeners of the lower fuselage region.

In order to substantiate the applied repair an initial comparative analysis was performed, comparing the main structural components near the damaged area, considering the original structure (without repair) and the modified structure (with repair). Later on, it was check the static mechanical behavior of the repair in order to check the structural integrity through the calculation of the margin of safety.

Figure 2. Details of the damaged fuselage

According to J. Tang et. Al (2013), the calculation accuracy of the FE method depends on the degree of approximation of physical characteristics of the model and its real structure. Therefore, a reasonable FE model of the center region of the aircraft was built, focusing on the damaged area, in order to carry out the FE analysis and optimization.

The process of Finite Element Analysis used in the study is shown in Figure 3. Firstly, a geometric model is generated using AUTODESK INVENTOR software. Secondly, the CAD model is imported in HYPERMESH, where the FE mesh is meticulously created. Then, the mesh is imported in Femap/NASTRAN where the properties of the components are set and desired loads and constraints are applied via manual software operations. Finally, with all parameters being set the analysis can run multiple times while adjusting the model conditions.

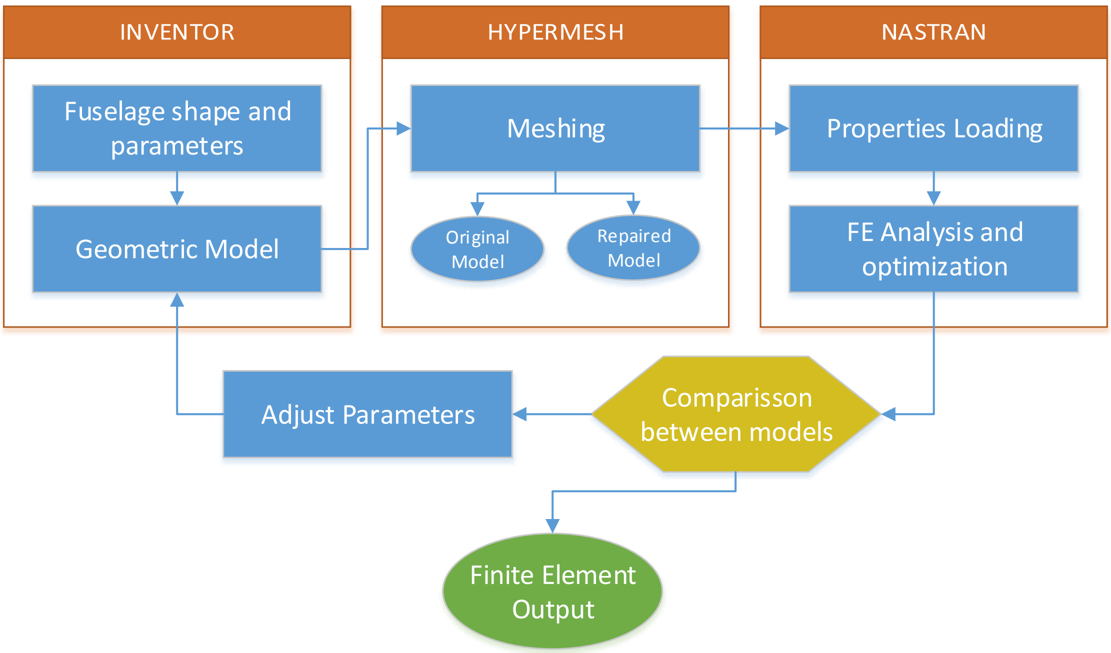

Figure 3. Process of finite element analysis

J. Tang et. Al (2013) also claims that aircraft structure design is an iterative process, therefore a new round of adjustment of the structure layout and repeated meshing and finite element property loading are needed in each iteration.

The evaluation in this paper is positioned in the analysis of a modification already done in the aircraft structure. After FE modeling completion, the definition of the repair structural design is formed, and the final FE analysis model and the optimized size parameters of the main components can be judged as acceptable or unacceptable for the safe operation of the aircraft.

2 FRAMEWORK TO REPAIR THE AIRCRAFT

The repair analyzed on this paper was originally projected following the design proposed in Figure 4. Here, the idea of reversed engineering is applied. Firstly, a simple repair project was design, where the main idea was to perform a large cut on the most affected panel, and cover it with a sheet of the same thickness attached by rivets to the main structural components. The repair is connected to the external face of the skin by to fillets of rivets on its border. Also, for the contact of the repair to the fuselage frames and stiffeners a slice of sheet was inserted between the components and fixed with rivets, in order to fulfill the space.

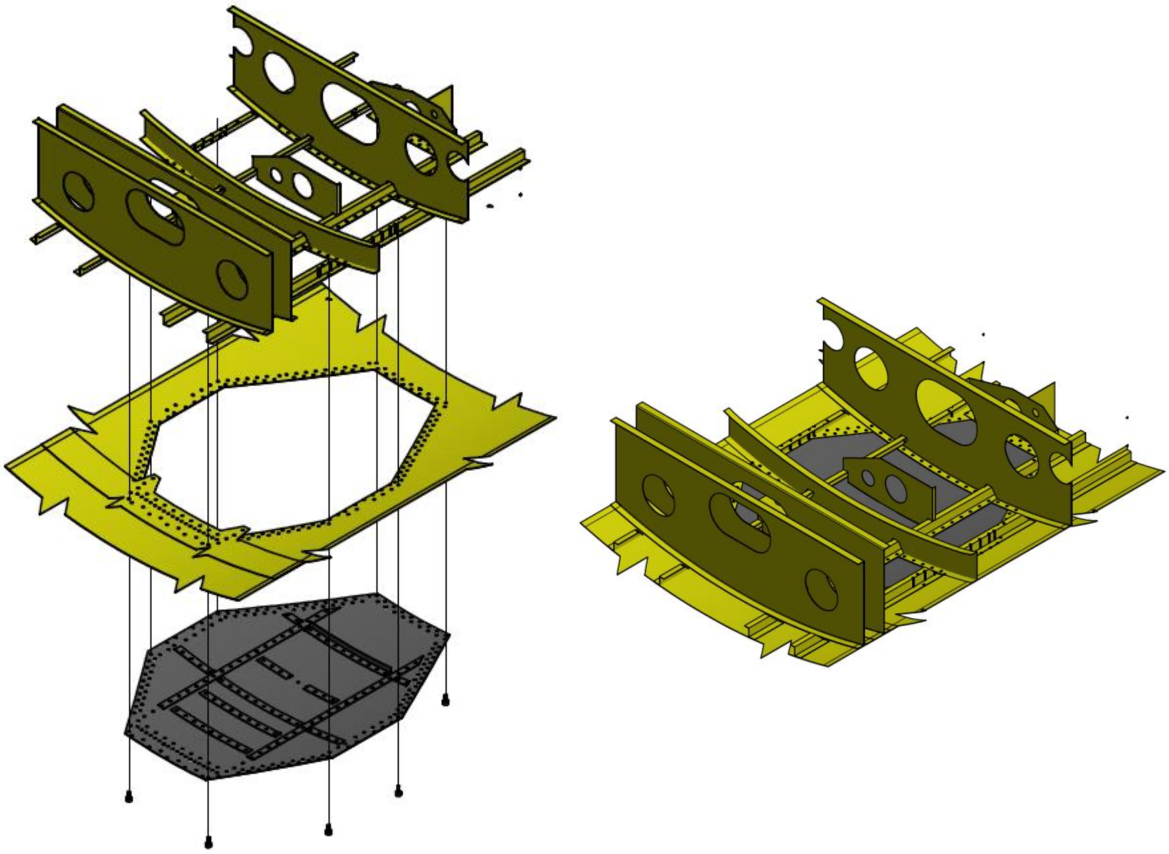

Figure 4. Project design of the repair

Figure 5 shows the stages of the work done on the real aircraft.

(1) (2) (3) (4)

Figure 5. Stages of the repair work

3 DESCRIPTION OF ORIGINAL AND REPAIRED MODELS

3.1 Geometric Model

Figure 6 shows the CAD model generated using AUTODESK INVENTOR software. It includes the fuselage's lower region with its main structural components located between fuselage frames C7 and C11 according to the manufacturer's manual.

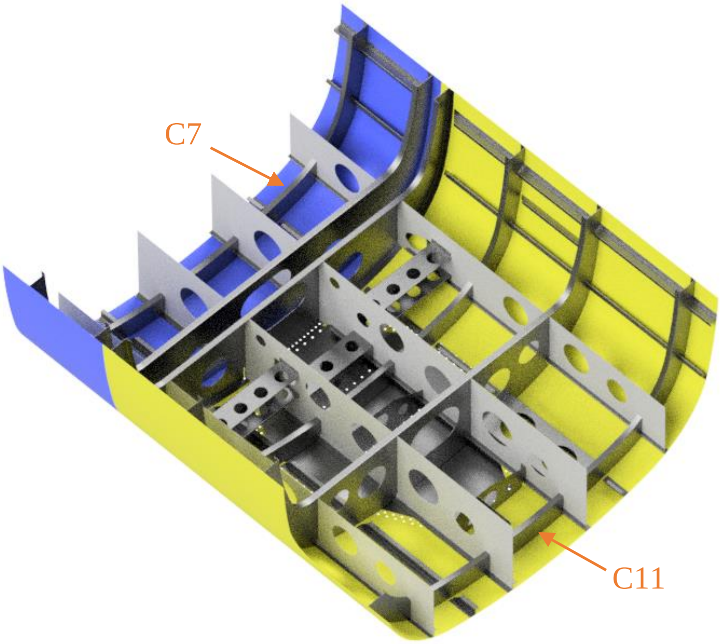

Figure 6. CAD model of the fuselage of the aircraft

The main components are described as follows:

3.1.1 Fuselage Frames

The fuselage frames were design of C beams with a height of 80 mm and upper and lower tabs of 20 mm each and some of them are used as the main support for the aircraft floor. They are all made of aluminum AL 2024-T3 with thickness 1.016 mm.

3.1.2 Fuselage Skin

The entire skin of the aircraft consists of aluminum panels AL 2024-T3 with 1.016 mm thick, which are arranged for fuselage, wings and stabilizers. In the region of analysis, there are only two panels. The junction is in the C8 fuselage frame where the wing is connected to the fuselage. One of the panels was the most affected component with the accident. A large cut was performed in order to remove damaged material.

3.1.3 Stiffeners

The stiffeners in the fuselage are composed of Z beams with a height of 30 mm and made of aluminum AL 2024-T3 with thickness 1.016 mm. Some of them go through the fuselage frames by small holes while others consist of short strips positioned between the frames.

3.1.4 Longitudinal beams

The longitudinal beams are composed by two pairs of sheets of aluminum AL 2024-T3 with 200 mm and 280 mm height, and serve as support for the floor inside the aircraft. They have a thickness of 1.016mm.

3.1.5 Supporters

The supporters are components serving as a support for mechanical and electronic components for various aircraft systems, but they also influence on the structural integrity of the aircraft. They are made of aluminum Al 2024-T3 with a thickness of 1.016 mm.

3.1.6 Repair

The repair was manufactured from an aluminum AL 2024-T3 sheet with a thickness of 1.016 mm, cut to the desired shape and fastened to the structural components of the aircraft by using rivets. Figure 7 shows a comparison between the real component and the CAD model used in the simulations.

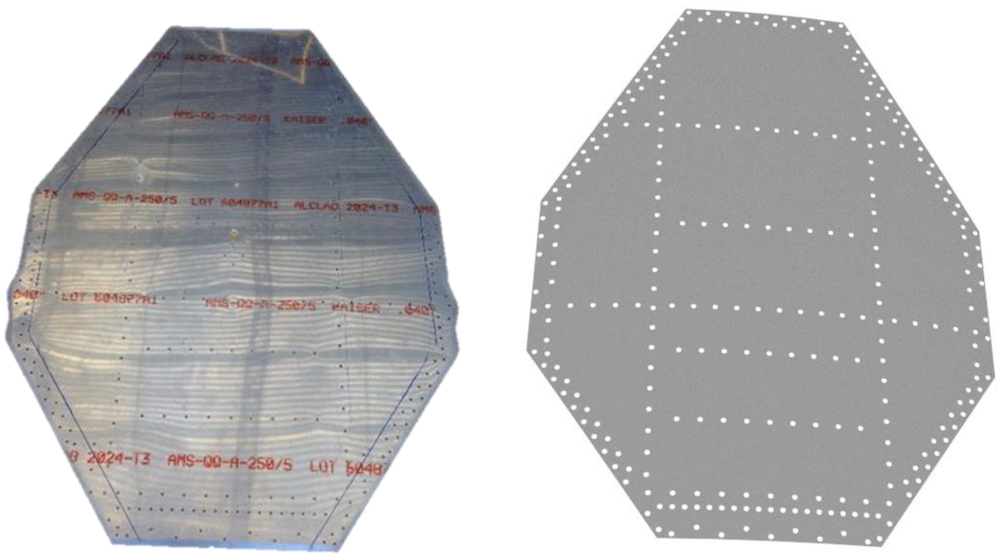

(a) **(b)**

Figure 7. Comparison between (a) real component and (b) CAD model

3.2 Finite Element Models

Both finite element models were built using plate elements of the type CTRIA3 and CQUAD4 for all the aircraft components, and for the rivets, spring/damper elements of the type CBUSH were used. The amount of elements in each component is shown below on Table 1.

Table 1. Finite Element Components Details for both models

Components	Number of Elements	Number of Nodes
Fuselage Frames	45857	48262
Stiffeners	12344	13856
Longitudinal Beams	32562	33898
Supporters	5324	5885
Doublers	765	928

As mentioned before two models were built in order to evaluate the structural integrity of the repaired aircraft. Therefore, there is a difference in the number of elements and nodes used in some of the components in each model. Details can be seen on Table 2.

Table 2. Finite Element Components Details for each model

	Repaired Model		Original Model	
	No. of Elements	No. of Nodes	No. of Elements	No. of Nodes
Fuselage Skin	57633	58355	66950	67390
Rivets	1232	2358	1032	2040
Repair skin	15876	16218	-	-

The finite element model for the repaired condition can be seen in details in Figure 8. As we can see, the region closest to the bottom of the fuselage has the most refined mesh, since that is the area of greatest interest.

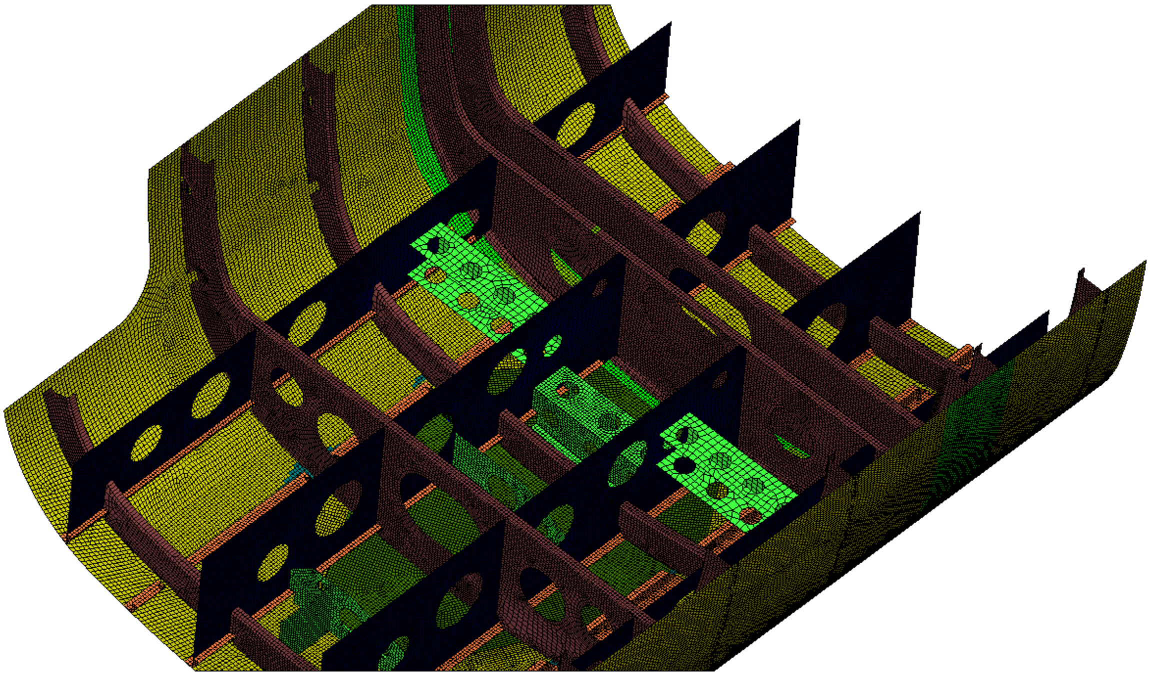

Figure 8. Finite element model of repaired aircraft

4 CERTIFICATION REQUIREMENTS

Work in this paper was based on the Brazilian requirements for airworthiness RBHA 23 that applies for this kind of aircraft. The requirements corresponds to the American FAR part 23 as shown below on Table 3.

RBHA 23 - Airworthiness Standards: Normal, utility, acrobatic and commuter category airplanes.

Table 3. Certification Requirements

Requirements	Description
FAR 23.303;	Factor of Safety
FAR 23.305 (a);	Strength and Deformation
FAR 23.365 (e)	Pressurized Compartment Loads
FAR 23.601;	General
FAR 23.603 (a),(b),(c);	Materials
FAR 23.605	Materials
FAR 23.607 (a),(b),(c);	Fasteners
FAR 23.613 (a),(b),(c),(d),(e)	Material Strength Properties and Design Values

5 STATIC ANALYSIS

The main purpose of this analysis is to simulate the pressurization loads acting on the fuselage according to the operating conditions established by the manufacturer and in compliance with the FAR 23 requirements, as described in Section 3 of this paper. At this stage, two analyzes are made: A comparative analysis between the two models (original and repaired), and finally a crimping analysis of the affected region to evaluate the loads applied to the rivets.

According to the aircraft manufacturer's manual, pressurization load operation of the TBM 700 is 6.2 psi. However according to FAR 23.365 the aircraft must withstand a 1.33 times the differential pressure above the operating pressurization:

$$\Delta P = 1{,}33 \times 6{,}2\ psi \quad (1)$$

$$\Delta P = 8{,}246\ psi \quad (2)$$

Therefore, firstly a static pressurization load of 8,246 psi is applied from the inside of the aircraft directed to the fuselage’s skin in both models. From the results it can be seen the distribution of loads among the aircraft’s structure analyzing the behavior and influence of the repair on the aircraft’s structural integrity.

One of the main active components in an aircraft structure are the rivets, they are able to withstand high values of load and enable the distribution of these loads throughout the structure preventing it to focus on a single region. In the second step, one crimping analysis is performed in order to get the maximum load values acting on the rivets on both finite element models, thus guaranteeing the integrity and reliability of the component.

5.1 Maximum stress on the repair

Figure 9 shows the stress distribution throughout the internal and external surfaces of the repair. It can be seen that the maximum stress for the internal surface is located close to the border of the component with a value of 305.5 MPa. For the external surface, the critical point is located far from the rivets with a value of 160.0 Mpa.

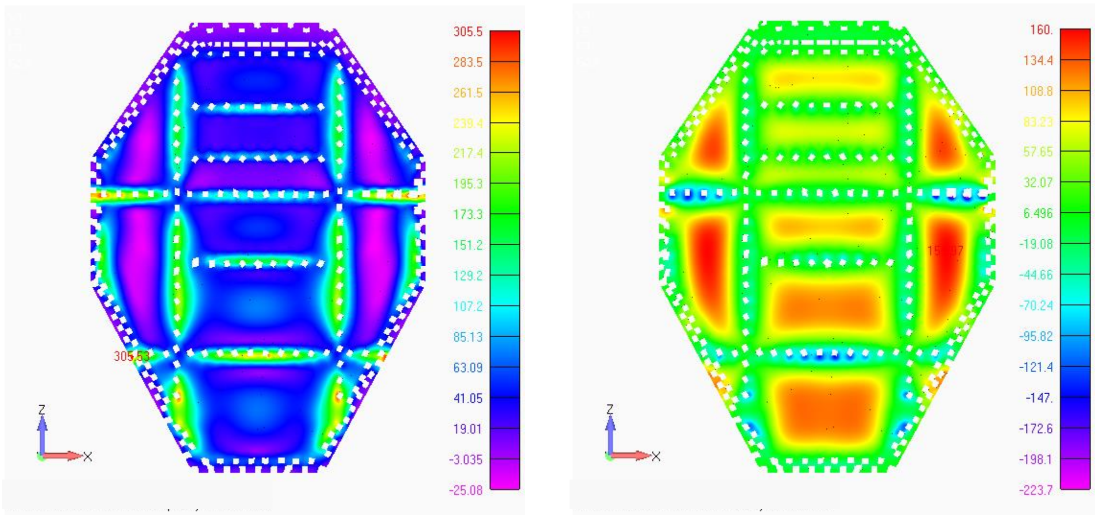

(a) (b)

Figure 9. Maximum stress on the repair (a) internal surface and (b) external surface

5.2 Crimping analysis in rivets

Figure 10 shows the results for crimping analysis performed, with the 10 most critical rivets located in the reparation region, with margins of safety of approximately 2.15.

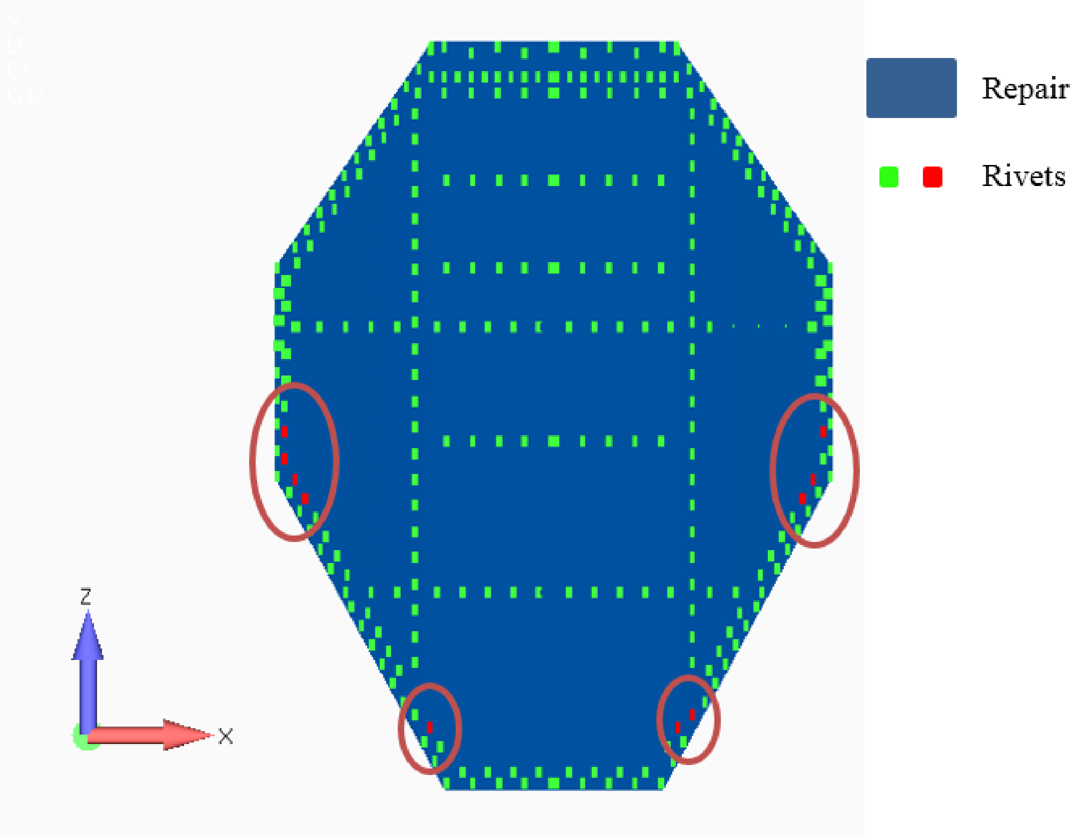

Figure 10. Most affected rivets with minimum margins of safety

According to the manufacturer of the rivets, to a sheet of 1.016 mm thickness, the maximum allowable shear and tension values are shown in Table 4.

Table 4. Properties of the rivets

Type	Dash	Thickness (mm)	Shear (N)	Tension (N)
MS14218AD	4	1.016	1430	1060

Therefore, using these data in the software, we can obtain the values for RT and RS for each rivet, and using the equation below the margin of safety can be estimated.

$$M.S. = \frac{1}{\sqrt{RT^2 + RS^2}} - 1 \tag{3}$$

5.3 Comparison of maximum stress in the skin

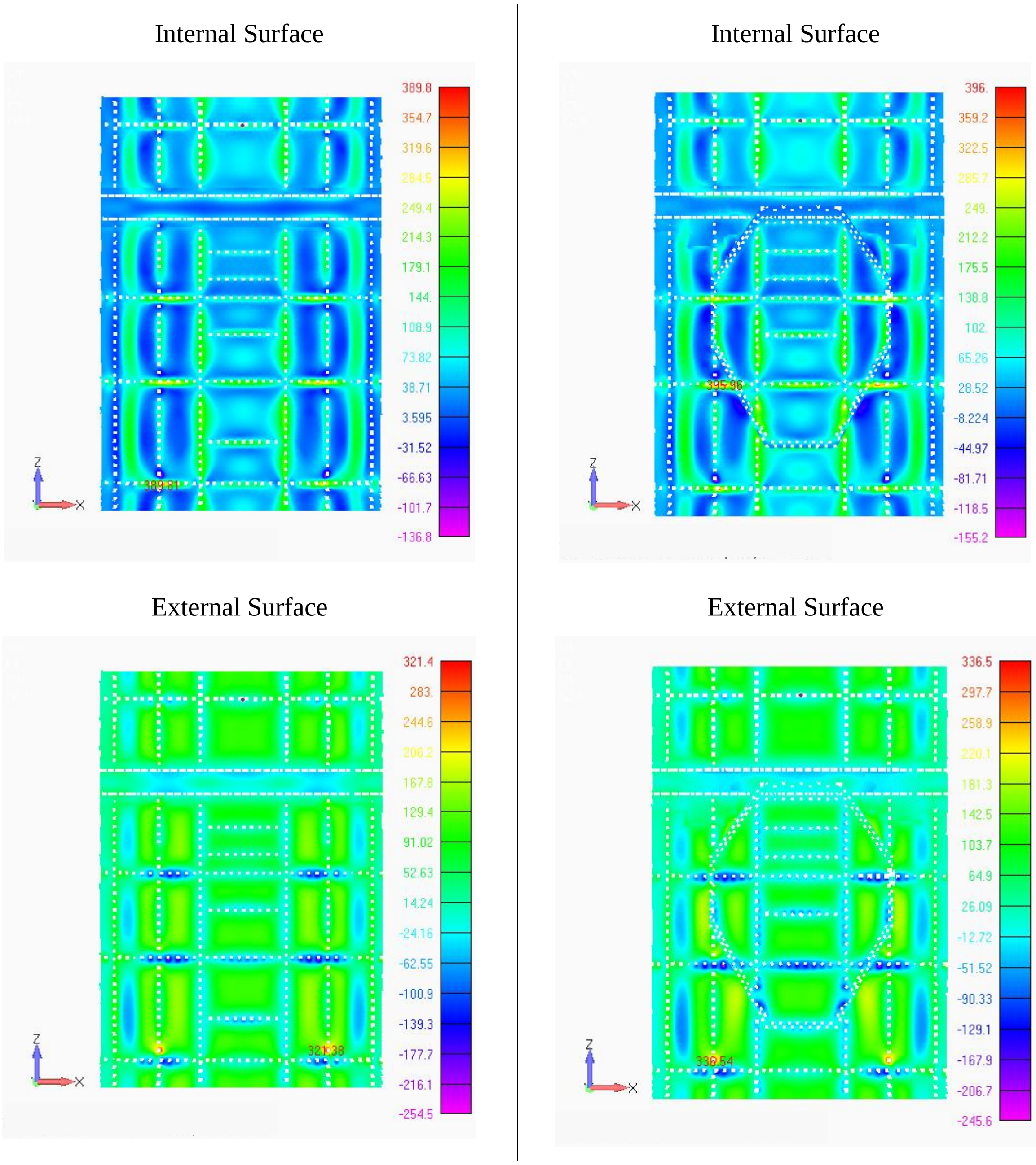

(a) **(b)**

Figure 11. Static Analysis – Skin (a) without repair and (b) with repair

With the repair, the maximum stress in the skin increased 1.5% in the internal surface and 4.7% in the external surface.

5.4 Comparison of maximum stress in the fuselage frames

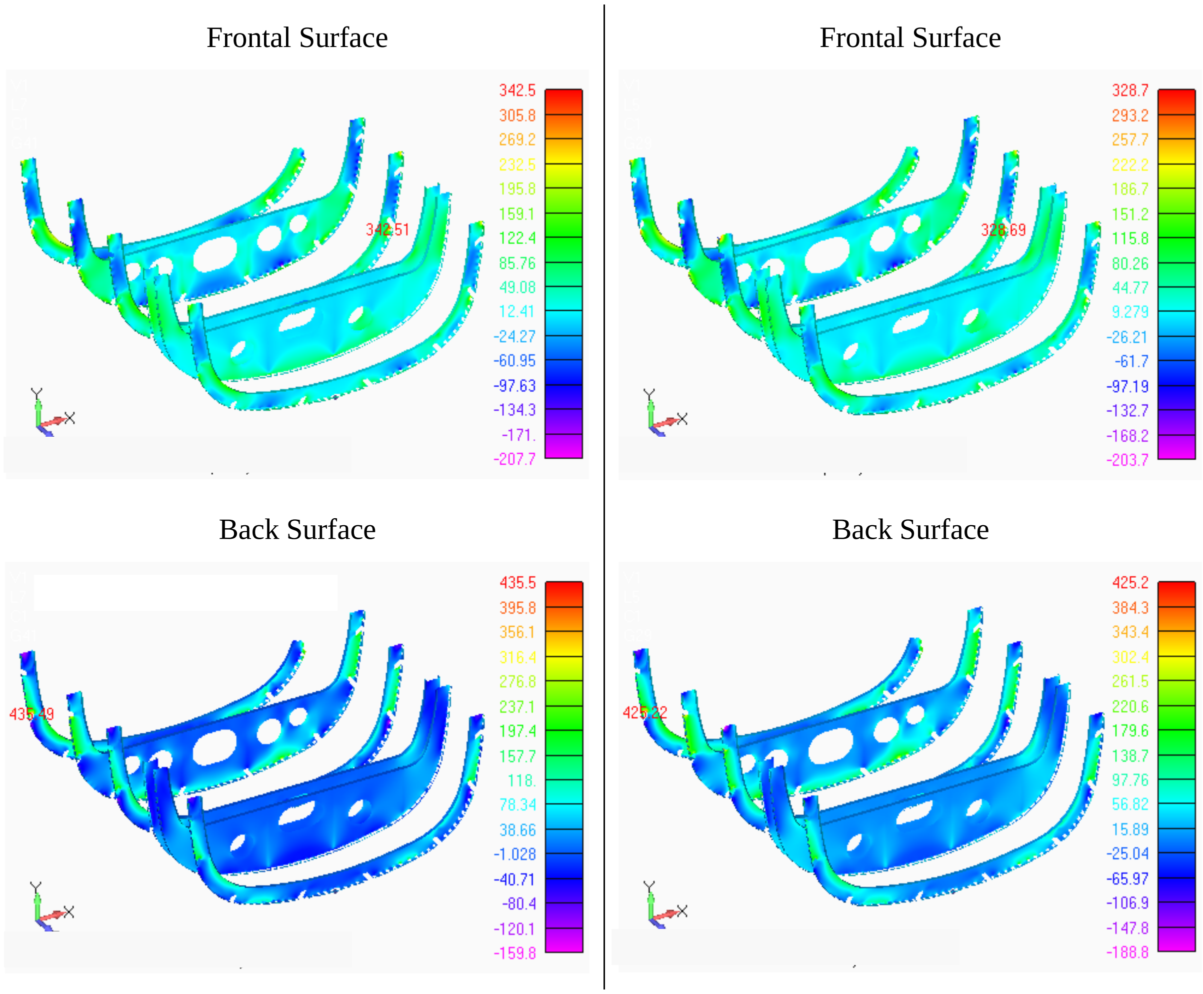

(a) **(b)**

Figure 12. Static Analysis – Fuselage frames (a) without repair and (b) with repair

With the repair, the maximum stress in the fuselage frames decreased 4.1% in the frontal surface and 2.4% in the back surface.

5.5 Comparison of maximum stress in the floor beams

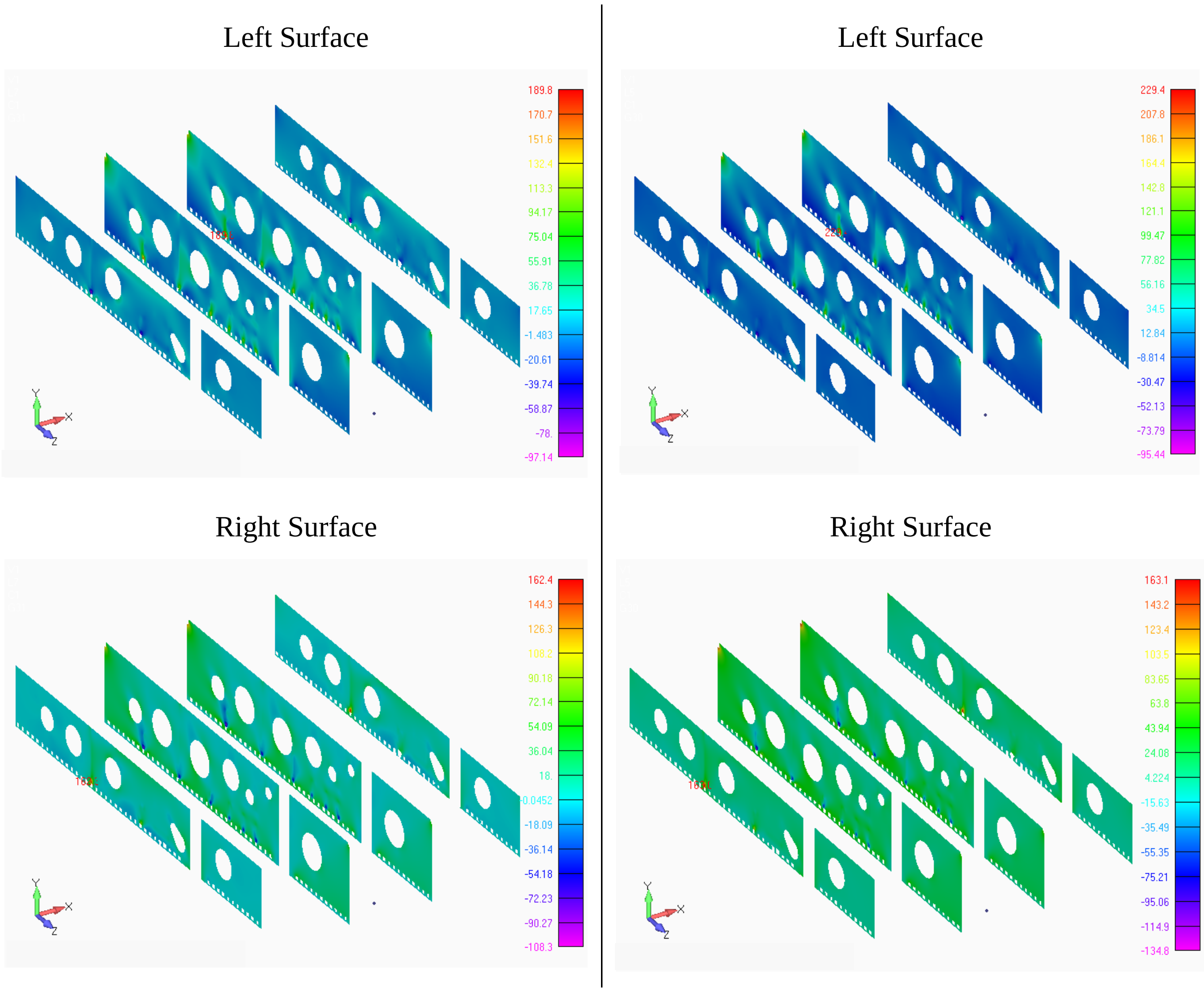

(a) **(b)**

Figure 13. Static Analysis - Floor beams (a) without repair and (b) with repair

With the repair, the maximum stress in the floor beams increased 20.8% in the left surface and 0.7% in the right surface.

6 RESULTS

The results of the comparison of the maximum tensions between the models with repair and without repair are presented in Table 5.

Table 5. Percentage of difference in the maximum stress value for aircraft with repair

Skin – External Surface	Increase	4,7%
Floor beams – Left Surface	Increase	20,8%
Fuselage frames – Frontal Surface	Decrease	4,1%

The results of the margin of safety for the repair, as well as the rivets in the repaired area are reported in Table 6 and Table 7, as shown below.

Table 6. Margin of safety for the repair skin

Part	Material	Load case	Failure Mode	Value [Mpa]	Allowable [Mpa]	S. M.
Repair skin	Al 2024-T3	8.22 psi	Yield Stress	305,5	310	1,014

Table 7. Margin of safety for the most critical rivets in the repair

Element	Load case	RT	RS	S. M.
7000089	8.22 psi	0.097	0.465	1.10
7000042	8.22 psi	0.117	0.451	1.14
7000038	8.22 psi	0.164	0.435	1.14
7000040	8.22 psi	0.164	0.431	1.16
7000090	8.22 psi	0.138	0.437	1.17
7000044	8.22 psi	0.112	0.444	1.18
7000113	8.22 psi	0.118	0.442	1.18
7000110	8.22 psi	0.111	0.437	1.21
7000116	8.22 psi	0.153	0.423	1.21
7000065	8.22 psi	0.093	0.439	1.22

7 CONCLUSION

A comparison between the original configuration of an aircraft and the repaired model is proposed in this paper. According to the results presented for the described pressurization loads, it can be concluded that the repair was designed properly, given the static criteria, since the margins of safety evaluated were positive for all components.

ACKNOWLEDGEMENTS

This work was supported by the University of Uberlandia in partnership with Algar aviation, which granted us with the workspace and all the equipment that we used.

REFERENCES

ALTAIR HYPERWORKS 13.0 student version

AUTODESK INVENTOR PROFESSIONAL 2016 student version

MSC/NASTRAN 2014 version

MilHandBook. Metallic materials and elements for aerospace vehicle structures.

Z.Q. Guan, Y.X. Gu, 2003. A parameterized method for 3D FE modeling based on CAD/CAE integration, *Computer Integration Manual System*, Volume 9.

Bruhn, E. F., 1973. Analysis and Design of Flight Vehicle Structures.

J. Tang, P. Xia, B. Zhanga, B. Hua, 2013. A finite element parametric modeling technique of aircraft wing structures, *Chinese Journal of Aeronautics* Volume 26.

L. Reimer, G. Wellmer, C. Braun, J. Ballmann, 2009. Computational Methods for Aero-Structural Analysis and Optimisation of Aircrafts Based on Reduced-Order Structural Models, *MEGADESIGN and MegaOpt - German Initiatives for Aerodynamic Simulation and Optimization in Aircraft Design*, Volume 107.

X.S. Sun, W.P. Chen, H.X. Chen, 1998. Design oriented FE modeling to aeronautical structures, *Acta Aeronautica et Astronautica Sinica*.

D.F. Anderson and S. Eberhardt, 2001. Understanding Flight. Ed. McGraw-Hill, New York, United States of America, 239 p.

M. C. Niu, 1996. Airframe Structural Design. *Hong Kong Conmilit Press Ltd*, Hong Kong, second edition.